

Solvates of a dianisyl-substituted donor–acceptor-type benzothiadiazole: mechanochromic, vapochromic, and acid-responsive multicolor luminescence

Takumi Yagi,^a Takashi Tachikawa^{b,c} and Suguru Ito^{*a,d}

^a Department of Chemistry and Life Science, Graduate School of Engineering Science, Yokohama National University
79-5 Tokiwadai, Hodogaya-ku, Yokohama 240-8501, Japan

*E-mail: suguru-ito@ynu.ac.jp

^b Department of Chemistry, Graduate School of Science, Kobe University,
1-1 Rokkodai-cho, Nada-ku, Kobe 657-8501, Japan

^c Molecular Photoscience Research Center, Kobe University,
1-1 Rokkodai-cho, Nada-ku, Kobe 657-8501, Japan

^d PRESTO, Japan Science and Technology Agency (JST),
4-1-8 Honcho, Kawaguchi, Saitama 332-0012, Japan

Table of contents

1. Fluorescence spectra of 1 in solution.....	S2
2. Single-crystal X-ray diffraction analyses.....	S3
3. Absorption spectra for crystalline 1 and 1•Solvent	S6
4. Theoretical calculations	S7
5. Fluorescence spectra for the MCL of 1•Solvent	S8
6. Powder X-ray diffraction (PXRD) patterns for the MCL of 1•Solvent	S11
7. ¹ H NMR spectra of 1•Benzene	S12
8. Supplemental data for the acid-responsive luminescence of 1•Pyridine	S13
Reference.....	S16
¹ H and ¹³ C NMR spectra.....	S17

1. Fluorescence spectra of **1** in solution

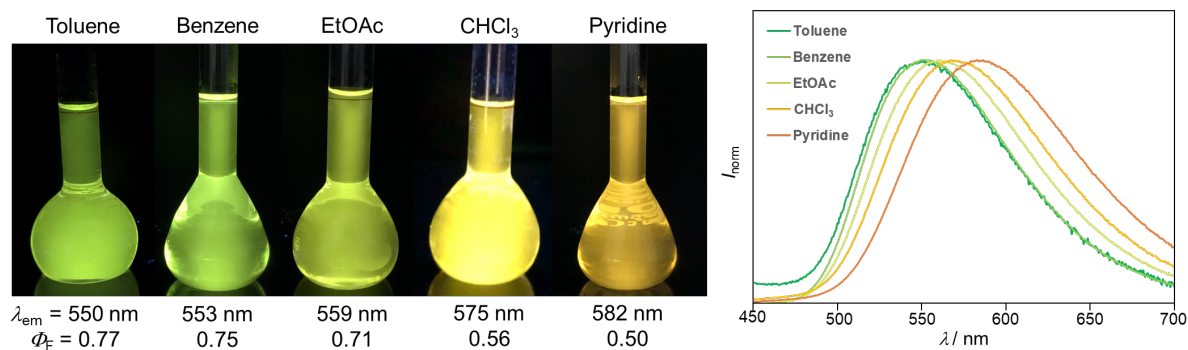


Fig. S1 Photographs and fluorescence spectra of **1** in solvents ($\lambda_{\text{ex}} = 365$ nm).

2. Single-crystal X-ray diffraction analyses

Table S1. Selected crystallographic data of **1** and **1•Solvent**

	1•CHCl₃	1•Benzene	1•Pyridine	1•EtOAc	1•Toluene	1
Empirical formula	C ₃₅ H ₂₄ N ₄ O ₂ S•CHCl ₃	C ₃₅ H ₂₄ N ₄ O ₂ S•C ₆ H ₆	C ₃₅ H ₂₄ N ₄ O ₂ S•C ₅ H ₅ N	C ₃₅ H ₂₄ N ₄ O ₂ S (+solvent)	C ₃₅ H ₂₄ N ₄ O ₂ S•C ₇ H ₈	C ₃₅ H ₂₄ N ₄ O ₂ S
Formula weight	684.04	642.75	643.76	564.66	656.80	564.66
Temperature / K	223	223.15	223	223	223	223
Crystal system	monoclinic	monoclinic	monoclinic	monoclinic	triclinic	triclinic
Space group	P2 ₁ /c (#14)	C2/c (#15)	P2 ₁ /c (#14)	P2 ₁ /c (#14)	P-1 (#2)	P-1 (#2)
<i>a</i> / Å	13.6322(2)	27.8666(4)	27.6505(2)	13.2848(2)	11.62224(9)	12.20306(9)
<i>b</i> / Å	22.3975(3)	10.41560(10)	10.34767(8)	21.9654(3)	14.66776(11)	21.16656(17)
<i>c</i> / Å	10.78060(19)	23.2099(4)	23.2526(2)	10.92692(17)	21.05256(16)	22.98109(18)
α / °	90.0000	90.0000	90.0000	90.0000	100.6593(6)	69.0121(7)
β / °	111.601(2)	108.110(2)	108.4906(10)	111.8702(18)	91.6602(6)	87.5755(6)
γ / °	90.0000	90.0000	90.0000	90.0000	109.9853(7)	87.6112(6)
<i>V</i> / Å ³	3060.44(9)	6402.89(17)	6309.54(9)	2959.06(8)	3297.98(5)	5534.93(8)
<i>Z</i>	4	8	8	4	4	8
<i>D</i> _{calcd} / g cm ⁻³	1.484	1.334	1.355	1.267	1.323	1.355
μ / mm ⁻¹	3.691	1.246	1.275	1.275	1.221	1.363
<i>F</i> (000)	1408.00	2688.00	2688.00	1176.00	1376.00	2352.00
Crystal size / mm ³	0.700 × 0.500 × 0.010	0.7 × 0.5 × 0.01	0.700 × 0.500 × 0.010	0.100 × 0.010 × 0.010	0.300 × 0.200 × 0.100	0.200 × 0.100 × 0.010
Radiation	CuKα (λ = 1.54184 Å)	CuKα (λ = 1.54184 Å)	CuKα (λ = 1.54184 Å)	CuKα (λ = 1.54184 Å)	CuKα (λ = 1.54184 Å)	CuKα (λ = 1.54184 Å)
2θ range for data collection / °	7.894 to 136.486	8.016 to 146.442	8.018 to 136.474	9.606 to 136.500	8.136 to 136.464	7.852 to 136.494
Index ranges	-16 ≤ <i>h</i> ≤ 16 -26 ≤ <i>k</i> ≤ 20 -12 ≤ <i>l</i> ≤ 10	-33 ≤ <i>h</i> ≤ 31 -12 ≤ <i>k</i> ≤ 12 -25 ≤ <i>l</i> ≤ 28	-33 ≤ <i>h</i> ≤ 31 -12 ≤ <i>k</i> ≤ 6 -27 ≤ <i>l</i> ≤ 28	-13 ≤ <i>h</i> ≤ 15 -26 ≤ <i>k</i> ≤ 25 -13 ≤ <i>l</i> ≤ 13	-13 ≤ <i>h</i> ≤ 14 -17 ≤ <i>k</i> ≤ 17 -25 ≤ <i>l</i> ≤ 22	-14 ≤ <i>h</i> ≤ 14 -23 ≤ <i>k</i> ≤ 25 -18 ≤ <i>l</i> ≤ 27
Reflections collected	18142	17502	19744	18511	46430	73764
Independent reflections	5603 [<i>R</i> _{int} = 0.0580]	6248 [<i>R</i> _{int} = 0.0459]	5778 [<i>R</i> _{int} = 0.0247]	5402 [<i>R</i> _{int} = 0.0288]	12036 [<i>R</i> _{int} = 0.0567]	20185 [<i>R</i> _{int} = 0.0323]
Data / restraints / parameters	5603/0/415	6248/0/401	5778/0/433	5402/0/379	12036/0/883	20185/0/1513
Goodness-of-fit on <i>F</i> ²	1.066	1.071	1.052	1.057	1.065	1.037
Final <i>R</i> indexes [<i>I</i> > 2σ(<i>I</i>)]	<i>R</i> ₁ = 0.0436, <i>wR</i> ₂ = 0.1219	<i>R</i> ₁ = 0.0533, <i>wR</i> ₂ = 0.1488	<i>R</i> ₁ = 0.0425, <i>wR</i> ₂ = 0.1126	<i>R</i> ₁ = 0.0425, <i>wR</i> ₂ = 0.1081	<i>R</i> ₁ = 0.0491, <i>wR</i> ₂ = 0.1362	<i>R</i> ₁ = 0.0608, <i>wR</i> ₂ = 0.1731
Final <i>R</i> indexes [all data]	<i>R</i> ₁ = 0.0470, <i>wR</i> ₂ = 0.1252	<i>R</i> ₁ = 0.0570, <i>wR</i> ₂ = 0.1521	<i>R</i> ₁ = 0.0449, <i>wR</i> ₂ = 0.1145	<i>R</i> ₁ = 0.0458, <i>wR</i> ₂ = 0.1106	<i>R</i> ₁ = 0.0533, <i>wR</i> ₂ = 0.1400	<i>R</i> ₁ = 0.0670, <i>wR</i> ₂ = 0.1783
Largest diff. peak/hole / eÅ ⁻³	0.26/-0.42	0.35/-0.43	0.48/-0.53	0.30/-0.54	0.54/-0.39	1.77/-0.61

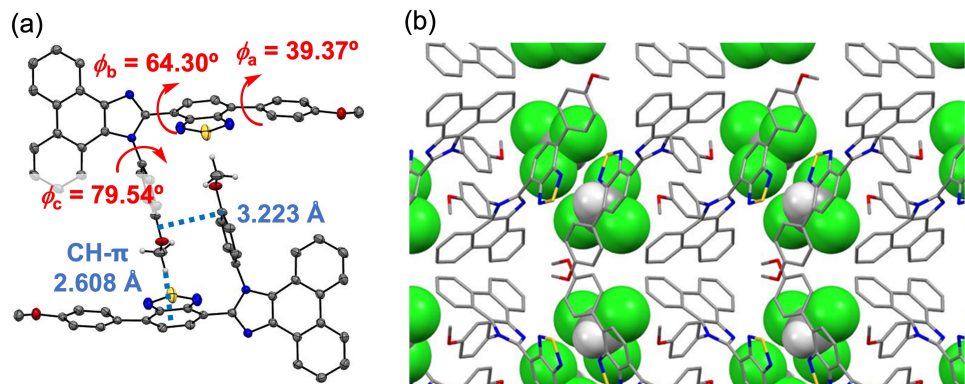


Fig. S2 The crystal structure of **1·CHCl₃** (Color code: gray = C, red = O, blue = N, yellow = S, green = Cl). (a) Adjacent two molecules with atomic displacement parameters set at 50% probability. (b) Packing structure. Solvate molecules are represented with space-filling model.

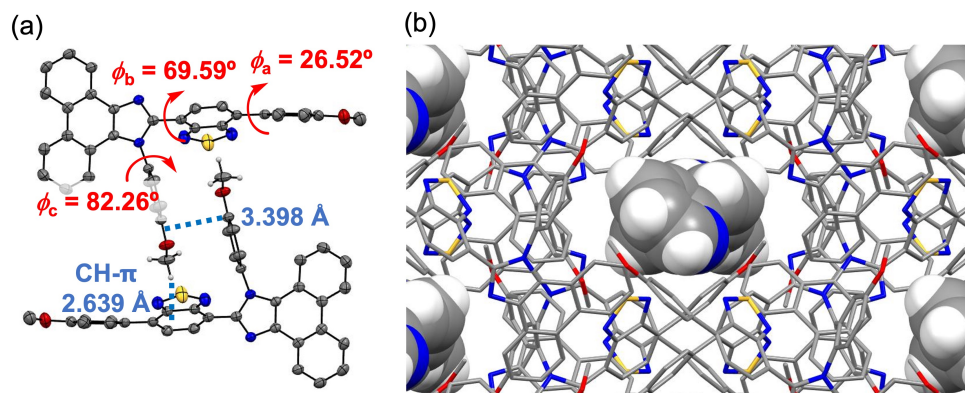


Fig. S3 The crystal structure of **1·Pyridine** (Color code: gray = C, red = O, blue = N, yellow = S). (a) Adjacent two molecules with atomic displacement parameters set at 50% probability. (b) Packing structure viewed along *c*-axis. Solvate molecules are represented with space-filling model.

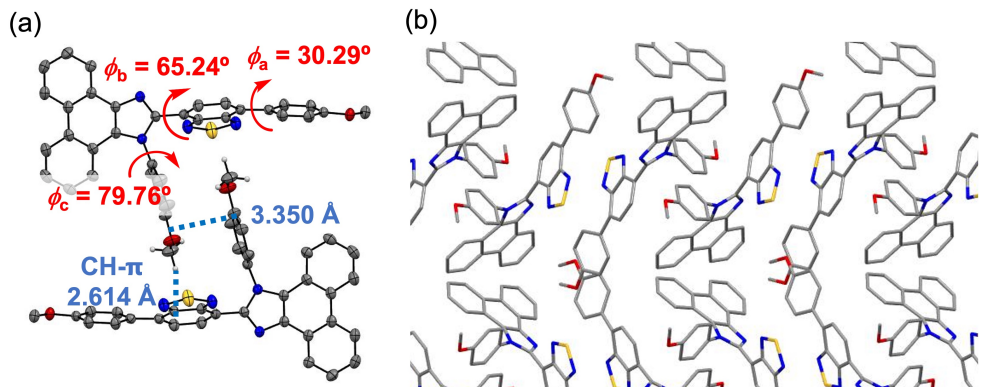


Fig. S4 The crystal structure of **1•EtOAc** (Color code: gray = C, red = O, blue = N, yellow = S). (a) Adjacent two molecules with atomic displacement parameters set at 50% probability. (b) Packing structure viewed along *c*-axis.

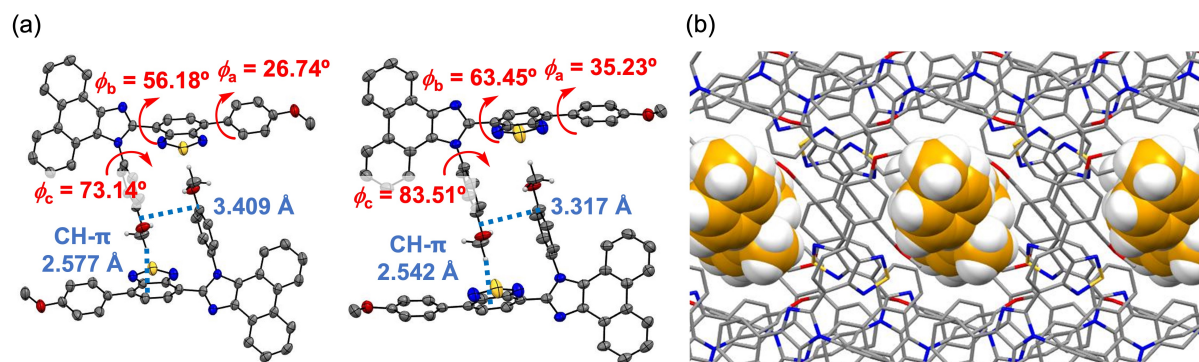


Fig. S5 The crystal structure of **1•Toluene** (Color code: gray = C, red = O, blue = N, yellow = S). (a) Adjacent two molecules with atomic displacement parameters set at 50% probability. Crystallographically independent two pairs are shown. (b) Packing structure viewed along *c*-axis. Solvate molecules are represented with space-filling model. Carbon atoms of solvate molecules are shown in orange.

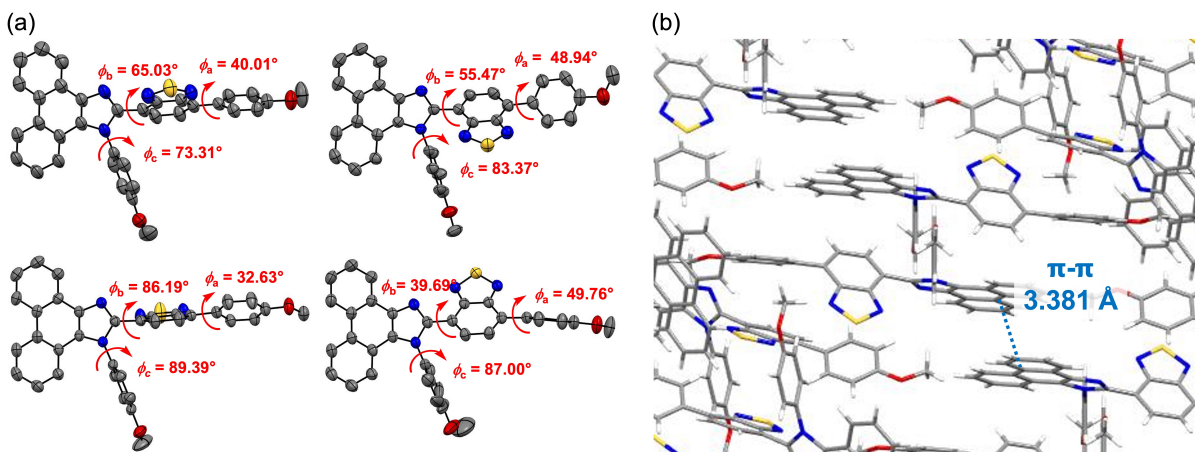


Fig. S6 The crystal structure of **1** with atomic displacement parameters set at 50% probability (Color code: gray = C, red = O, blue = N, yellow = S). (a) Four crystallographically independent molecules of **1**. (b) Packing structure of **1**.

3. Absorption spectra for crystalline **1** and **1**•Solvent

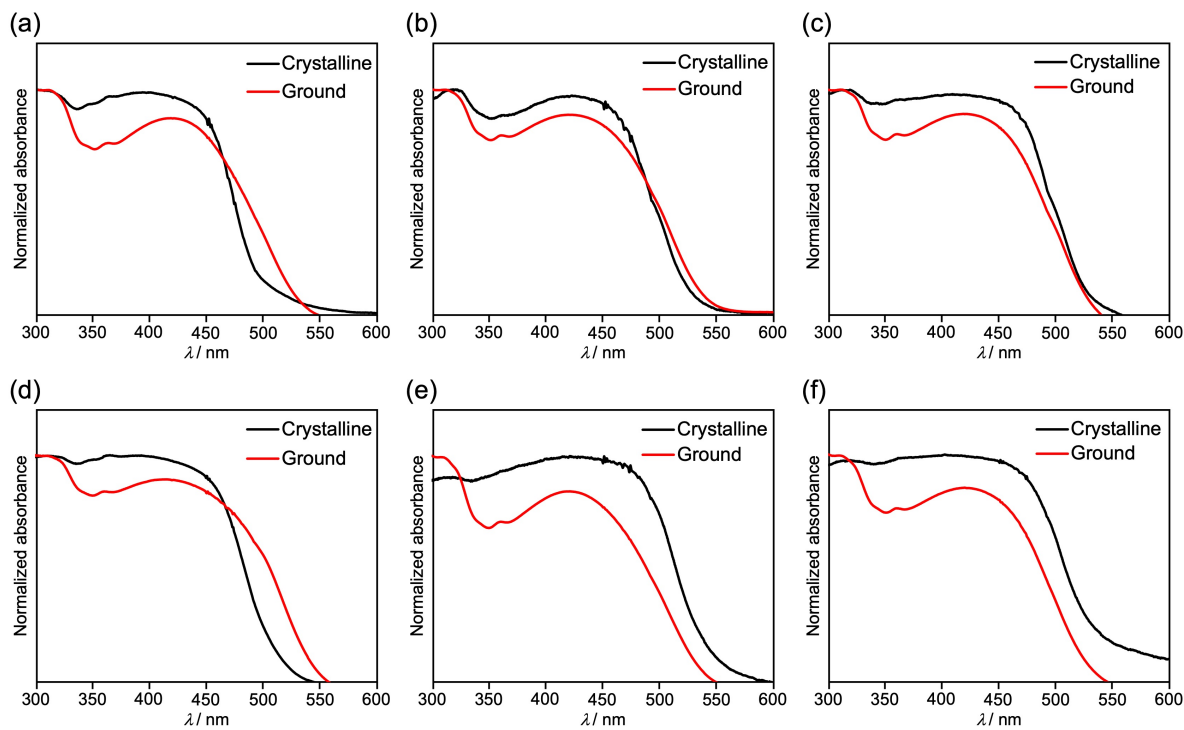


Fig. S7 Solid-state absorption spectra of **1**•CHCl₃ (a), **1**•Benzene (b), **1**•Pyridine (c), **1**•EtOAc (d), **1**•Toluene (e), and **1** (f).

4. Theoretical calculations

Table S2 Experimental fluorescence maxima and calculated absorption properties of X-ray structures for **1** and **1•Solvent**.

Compd.	Crystalline λ_{em} (nm)	Calcd λ_{abs} (nm)	Transition from HOMO to LUMO	Oscillator strength	HOMO (eV)	LUMO (eV)	Dipole moment (D)
1•CHCl₃	508	373	0.622	0.390	-6.37	-1.17	5.03
1•Benzene	521	379	0.607	0.422	-6.36	-1.19	5.20
1•Pyridine	522	377	0.607	0.408	-6.37	-1.20	5.23
1•EtOAc	524	381	0.614	0.428	-6.36	-1.20	5.25
1•Toluene	565	382	0.624	0.471	-6.35	-1.18	5.23
1	550	371	0.640	0.396	-6.42	-1.17	3.34

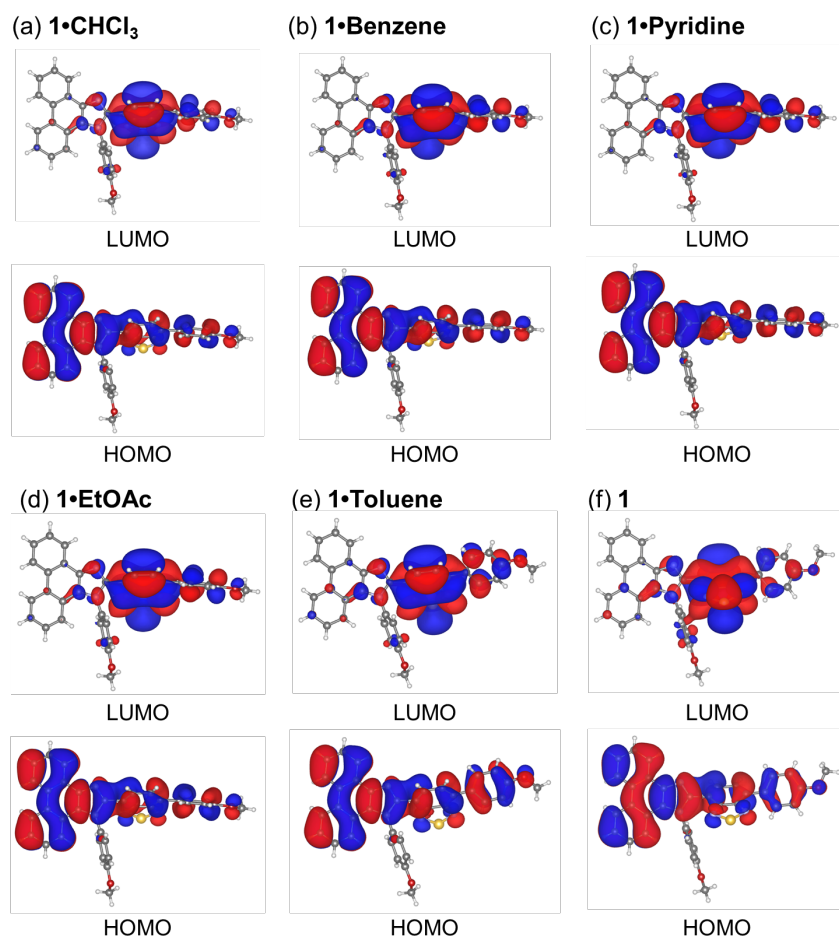


Fig. S8 HOMO and LUMO of **1** in crystalline **1•CHCl₃** (a), **1•Benzene** (b), **1•Pyridine** (c), **1•EtOAc** (d), **1•Toluene** (e), and **1** (f) calculated at the CAM-B3LYP/6-31G(d) level. The structures are drawn by VESTA.¹

5. Fluorescence spectra for the MCL of **1**•Solvent

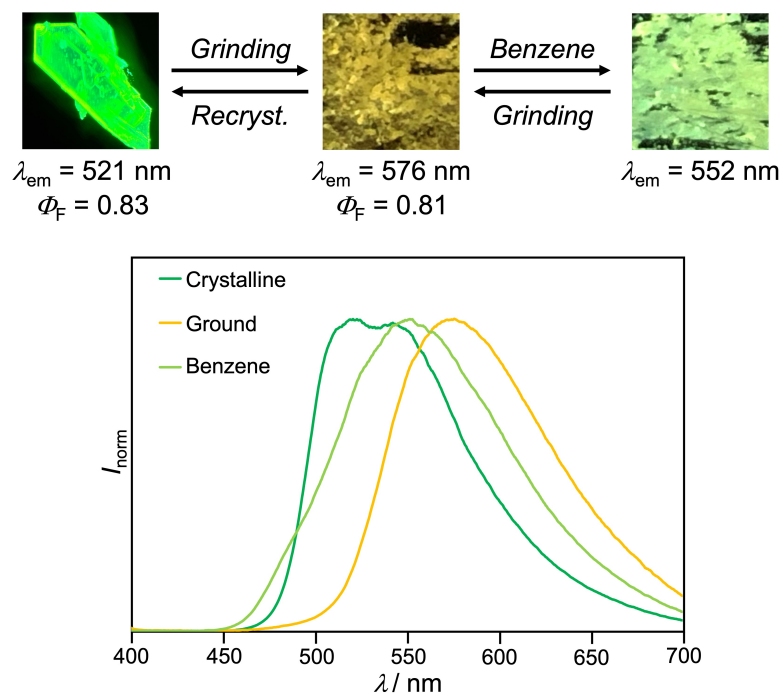


Fig. S9 Photographs and fluorescence spectra for the MCL of **1**•Benzene.

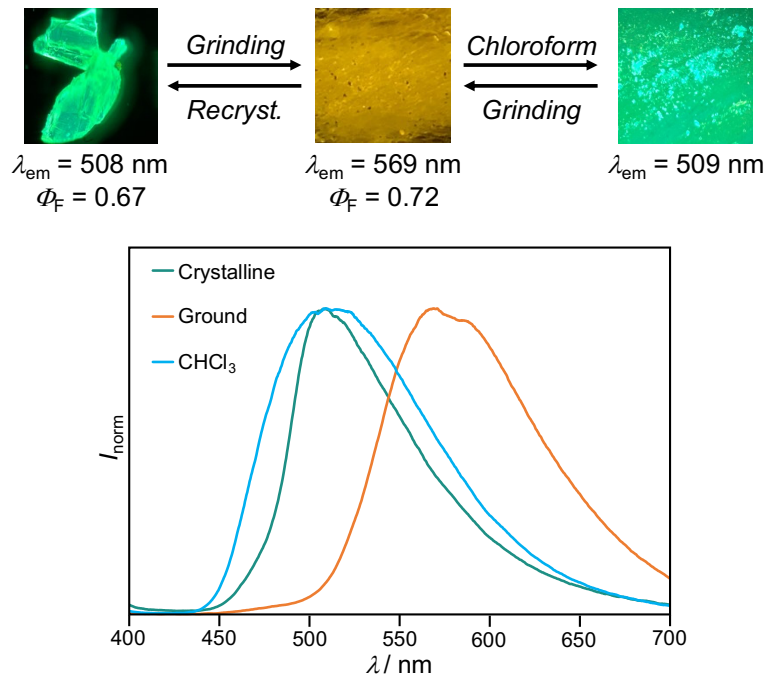


Fig. S10 Photographs and fluorescence spectra for the MCL of **1**•CHCl₃.

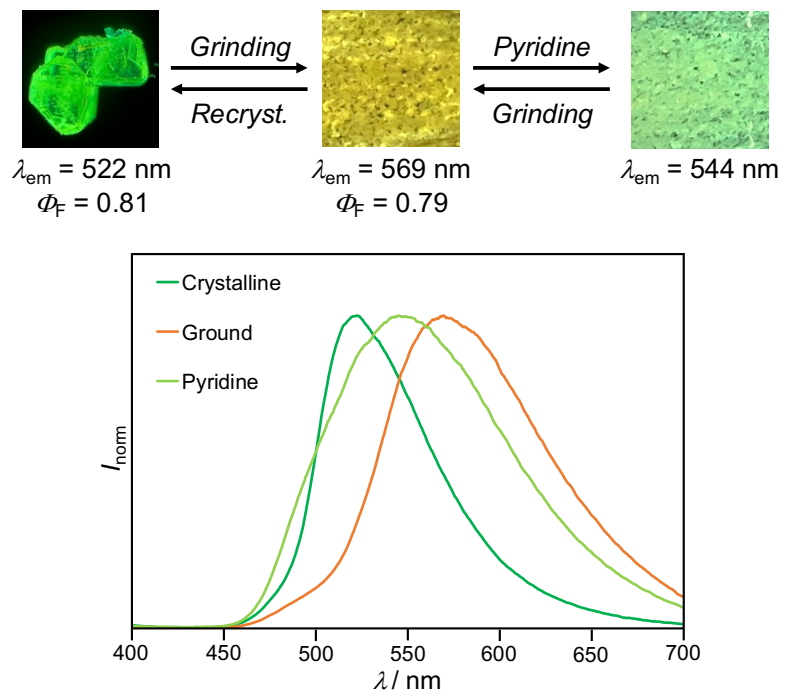


Fig. S11 Photographs and fluorescence spectra for the MCL of **1•Pyridine**.

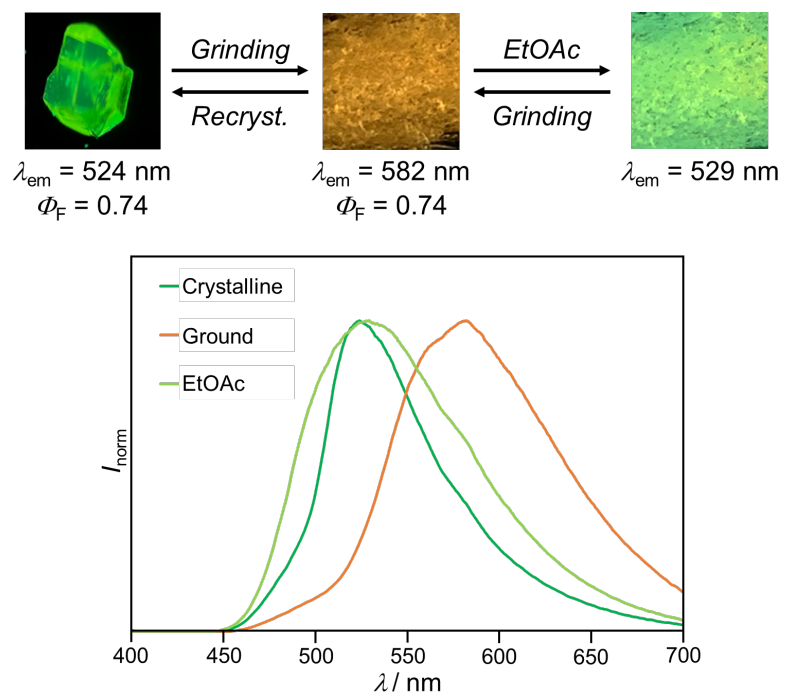


Fig. S12 Photographs and fluorescence spectra for the MCL of **1•EtOAc**.

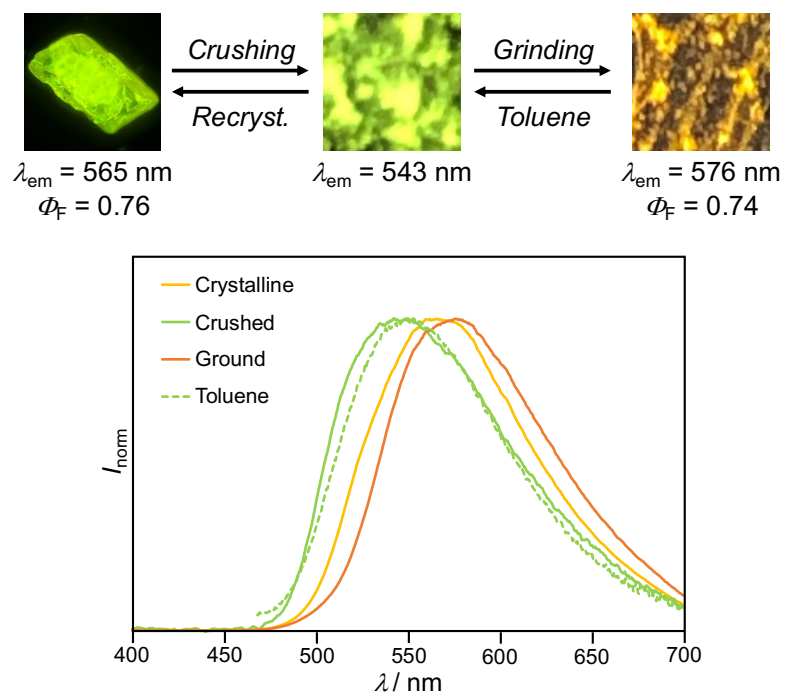


Fig. S13 Photographs and fluorescence spectra for the MCL of **1**•Toluene.

6. Powder X-ray diffraction (PXRD) patterns for the MCL of 1•Solvent

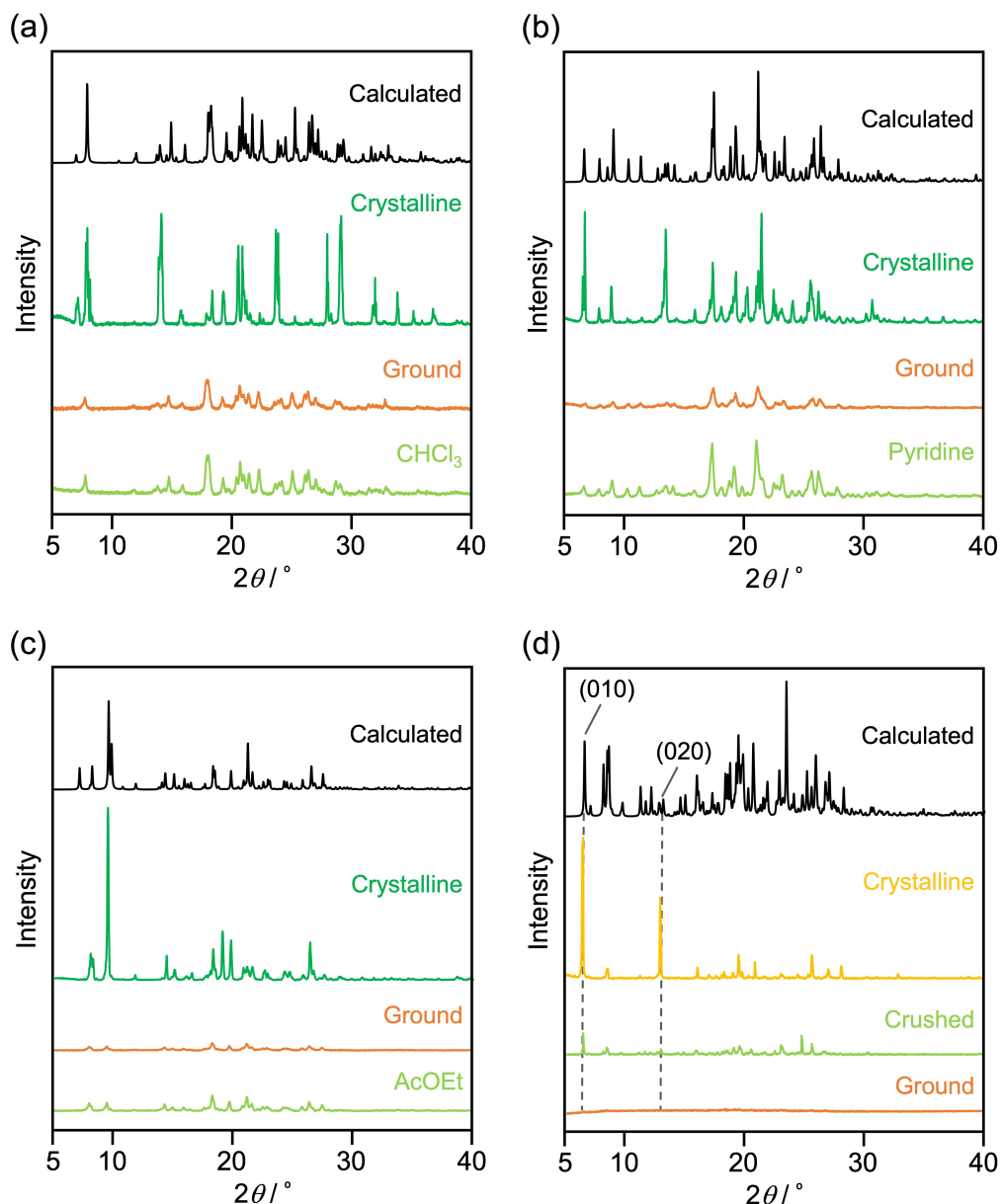


Fig. S14 PXRD patterns for **1•CHCl₃** (a), **1•Pyridine** (b), **1•EtOAc** (c), and **1•Toluene** (d). (a–c) Black lines: Simulated PXRD patterns calculated from the single-crystal structure. Green lines: Experimental PXRD patterns of the powdered crystalline samples. Orange lines: Experimental PXRD patterns of the ground samples. Yellow-green lines: Experimental PXRD patterns of the solvent-exposed samples. (d) Black line: Simulated PXRD patterns calculated from the single-crystal structure. Yellow line: Experimental PXRD patterns of the powdered crystalline sample. Yellow-green line: Experimental PXRD patterns of the crushed sample. Orange line: Experimental PXRD patterns of the ground sample.

7. ^1H NMR spectra of 1•Benzene

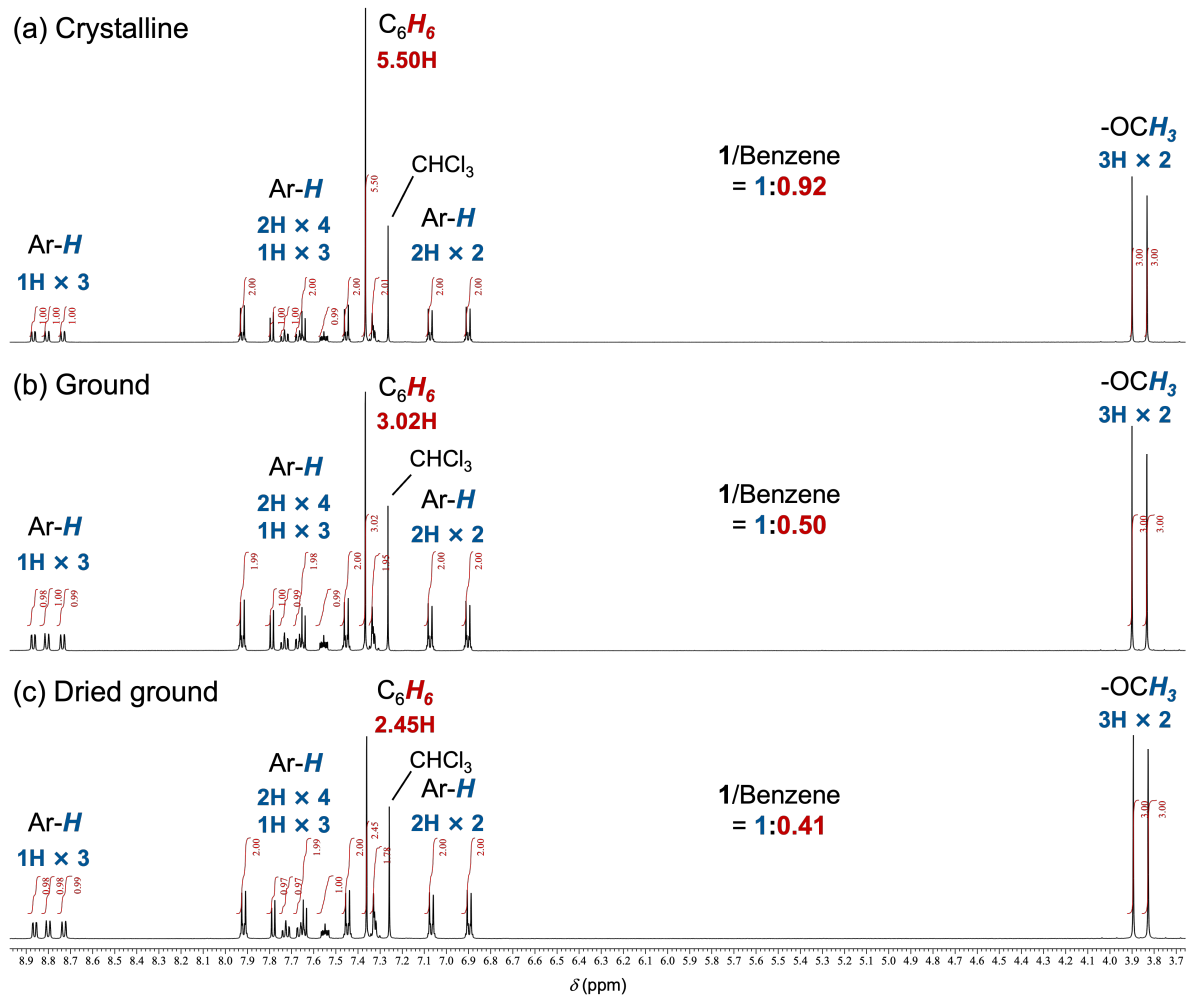


Fig. S15 ^1H NMR spectra (500 MHz, in CDCl_3 , rt) of (a) crystalline 1•Benzene, (b) ground 1•Benzene, and (c) ground 1•Benzene after drying in vacuo for 6 h.

8. Supplemental data for the acid-responsive luminescence of **1•Pyridine**

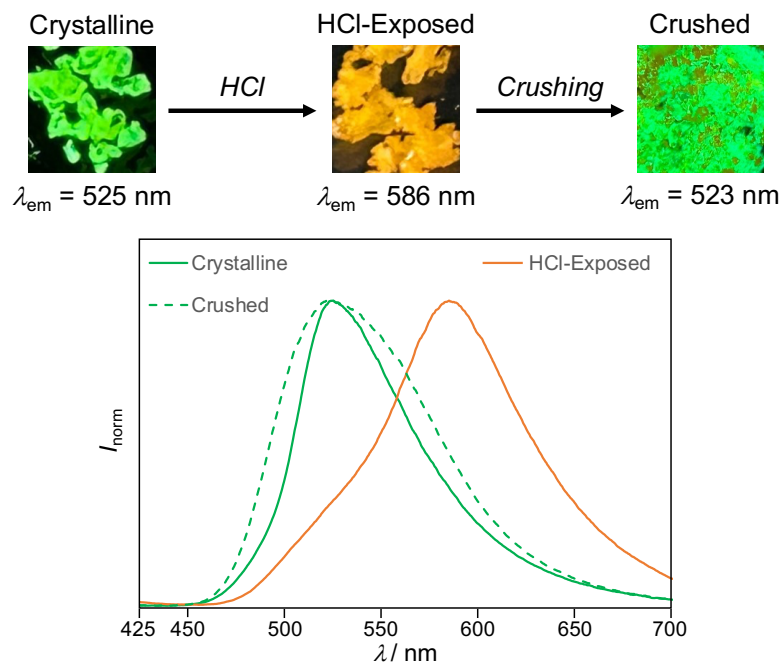


Fig. S16 Photographs and fluorescence spectra for acid-responsive luminescence of **1•Pyridine**.

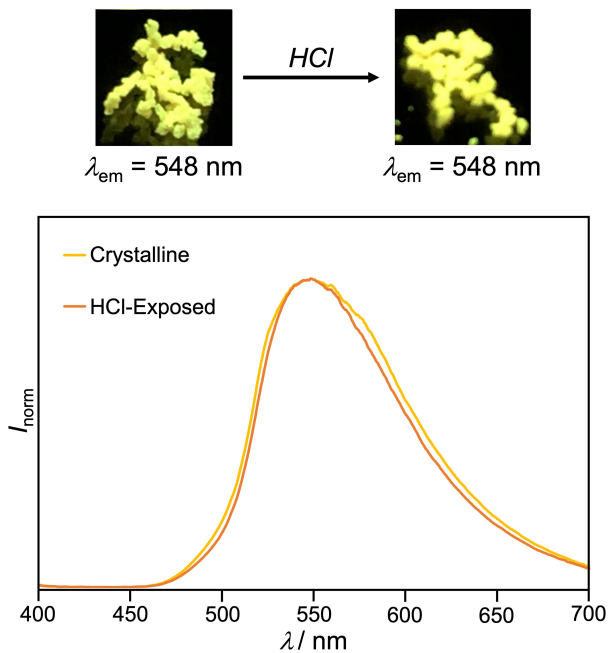
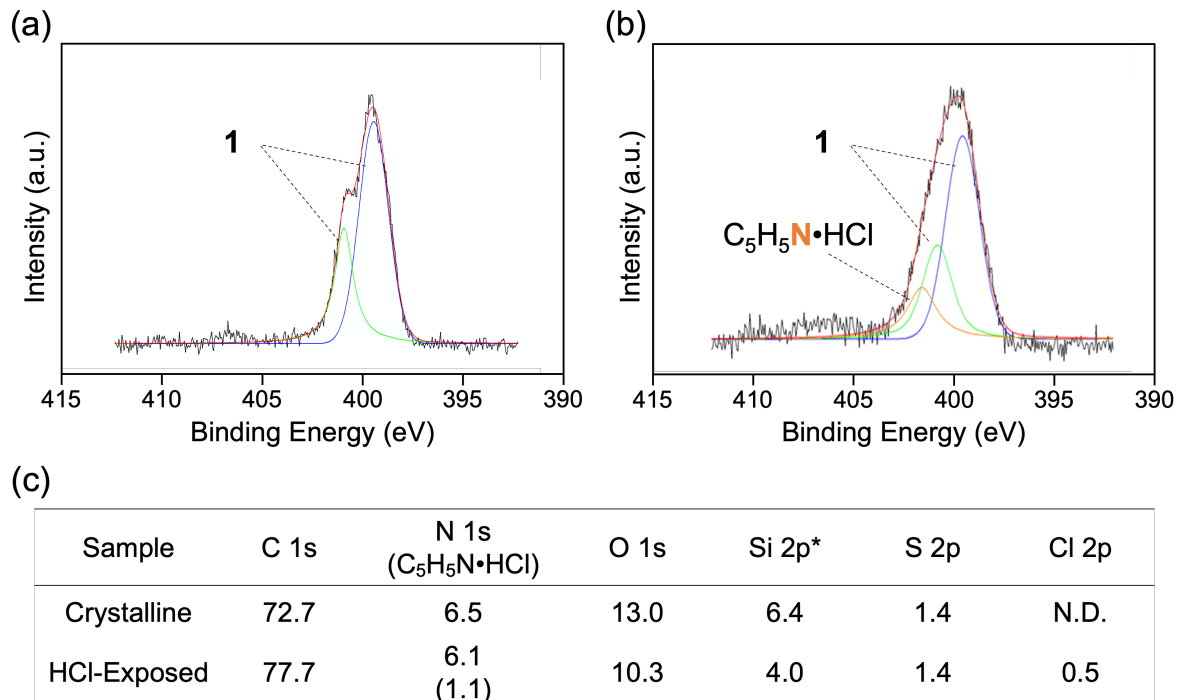


Fig. S17 Photographs and fluorescence spectra for crystalline **1** and acid-exposed **1**.

X-ray photoelectron spectroscopy (XPS) suggested the presence of pyridine hydrochloride on the surface of HCl-exposed **1•Pyridine** (Fig. S18). Surface pyridine molecules should have volatilized from crystalline **1•Pyridine** prior to XPS measurement under high vacuum conditions (Fig. S18a), while a broad N 1s peak that should correspond to protonated pyridine salts was detected for the HCl-exposed sample (Fig. S18b). In addition, Cl 2p was detected for HCl-exposed **1•Pyridine** (Fig. S18c).



*Derived from contamination.

Fig. S18 N 1s XPS spectra of crystalline **1•Pyridine** (a) and HCl-exposed **1•Pyridine** (b). (c) Atomic percentages (%) of the elements calculated from the XPS spectra of crystalline and HCl-exposed **1•Pyridine**.

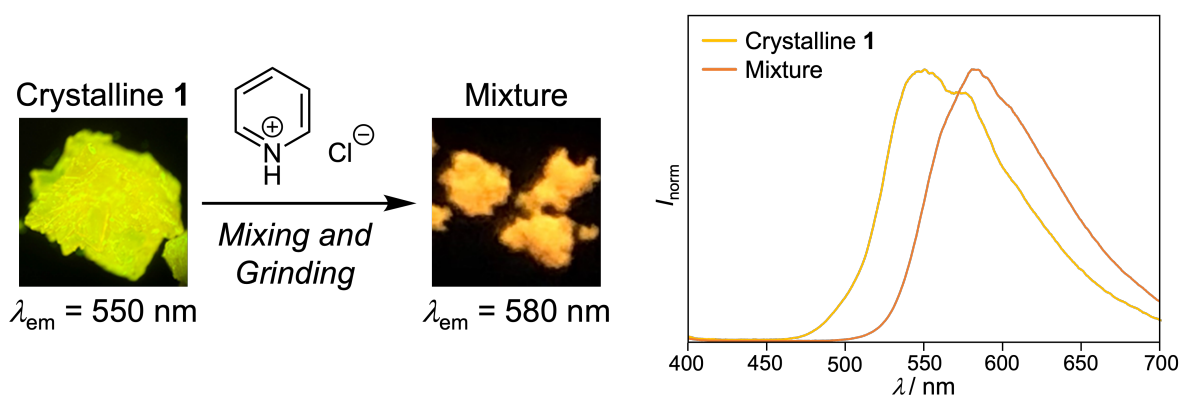


Fig. S19 Photographs and fluorescence spectra for crystalline **1** and mixture of **1** and pyridine hydrochloride.

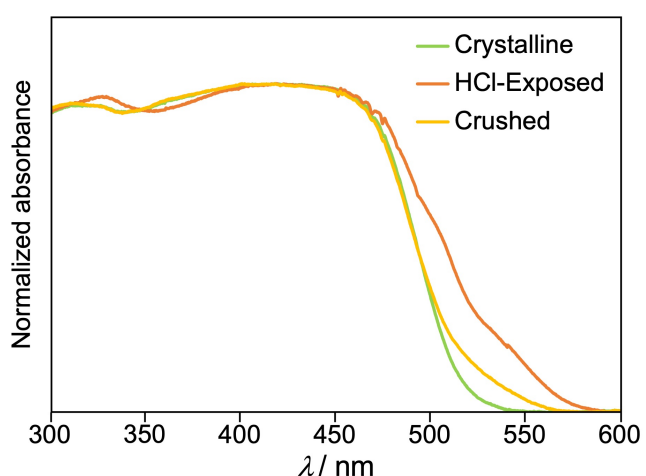


Fig. S20 Solid-state absorption spectra of crystalline, HCl-exposed, and crushed **1•Pyridine**.

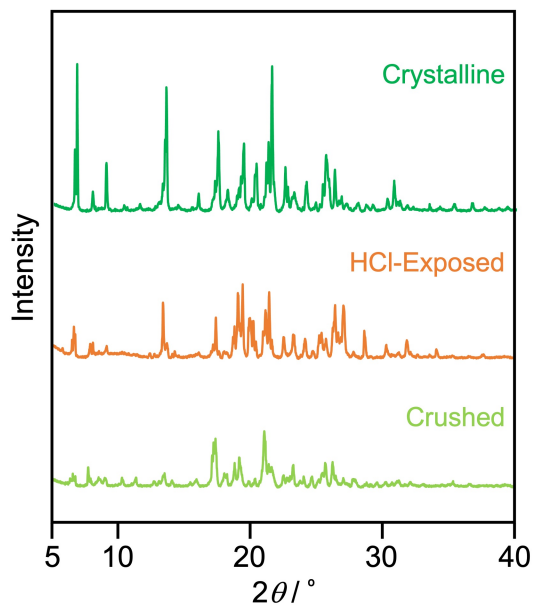


Fig. S21 PXRD patterns of **1•Pyridine**. Green line: Experimental PXRD pattern of the powdered crystalline sample. Orange line: Experimental PXRD pattern of the HCl-exposed sample. Yellow-green line: Experimental PXRD pattern of the crushed samples.

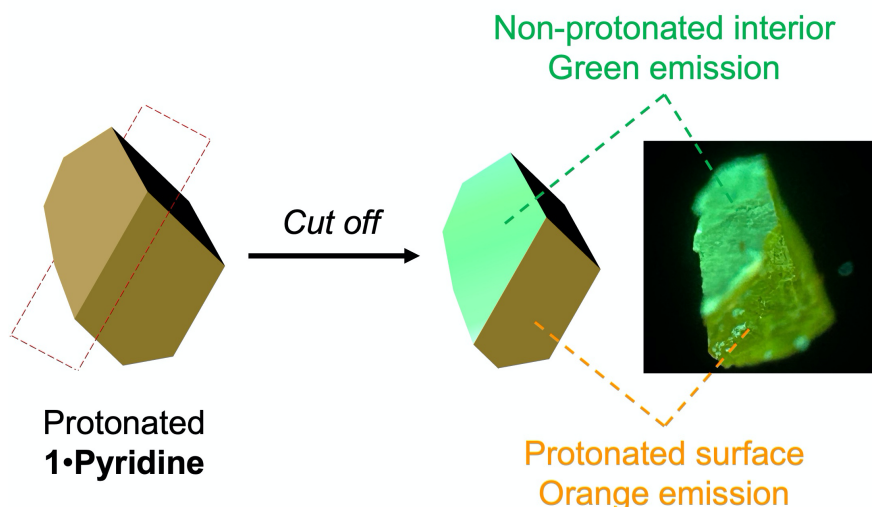
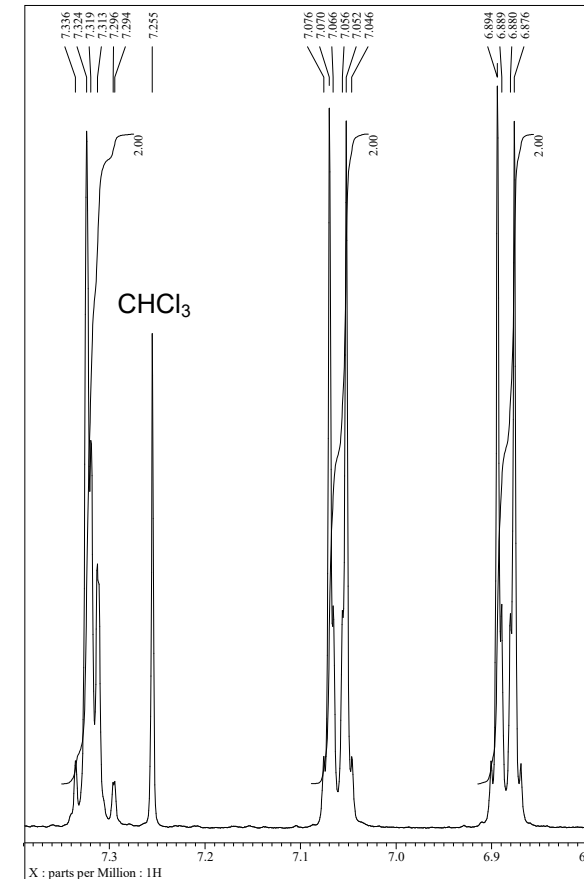
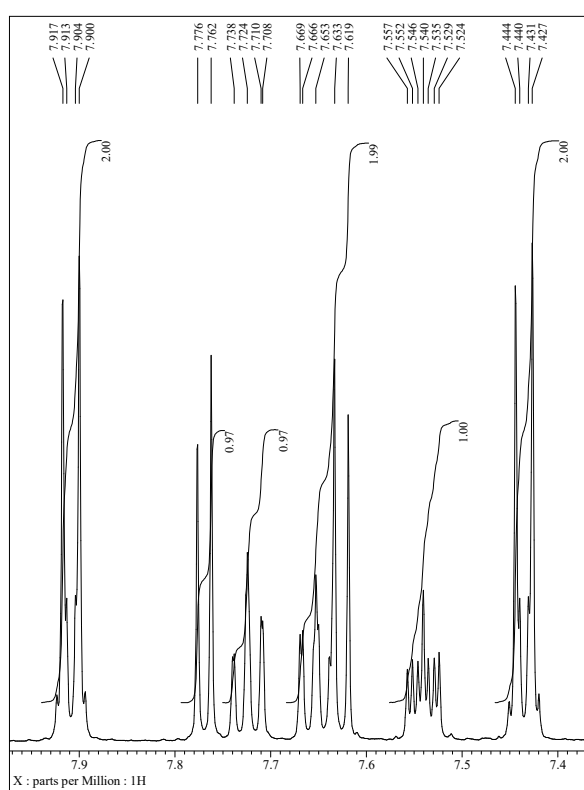
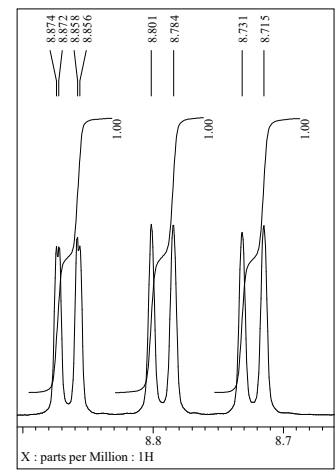
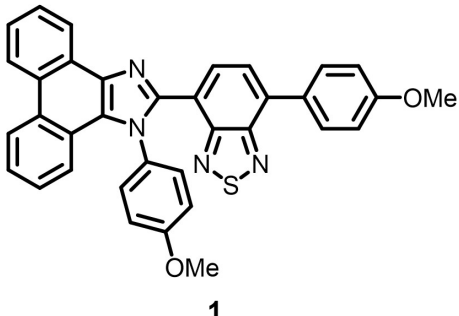


Fig. S22 Schematic diagram and photograph for the cutting process of HCl-exposed **1•Pyridine**.

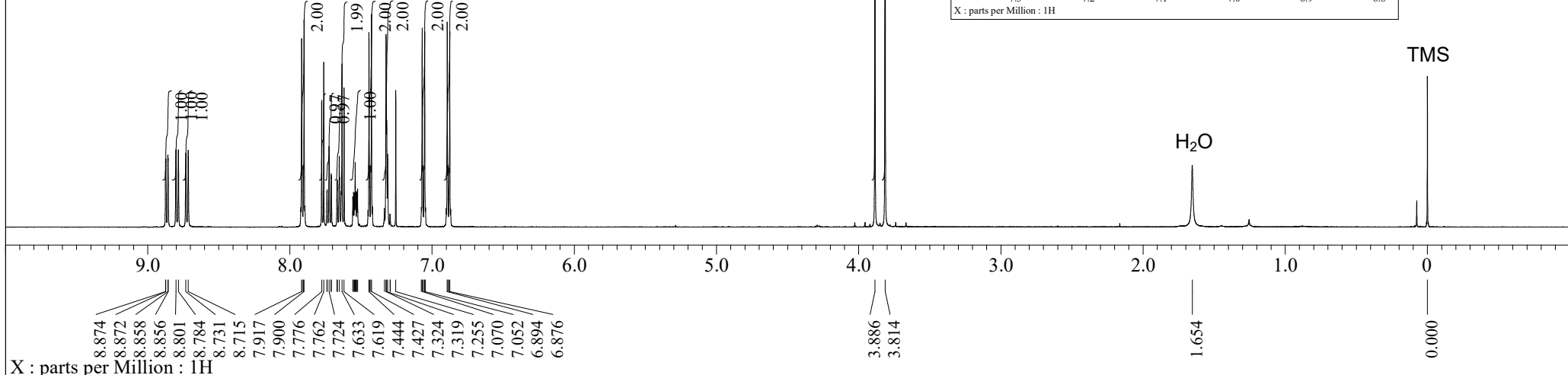
Reference

- 1) K. Momma and F. Izumi, *J. Appl. Crystallogr.*, 2011, **44**, 1272.

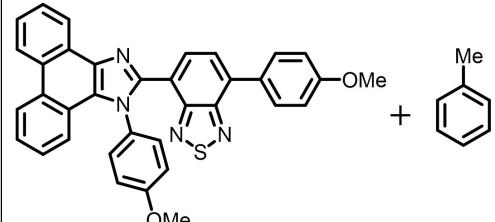
¹H NMR spectrum of **1** (500 MHz, CDCl₃, rt)



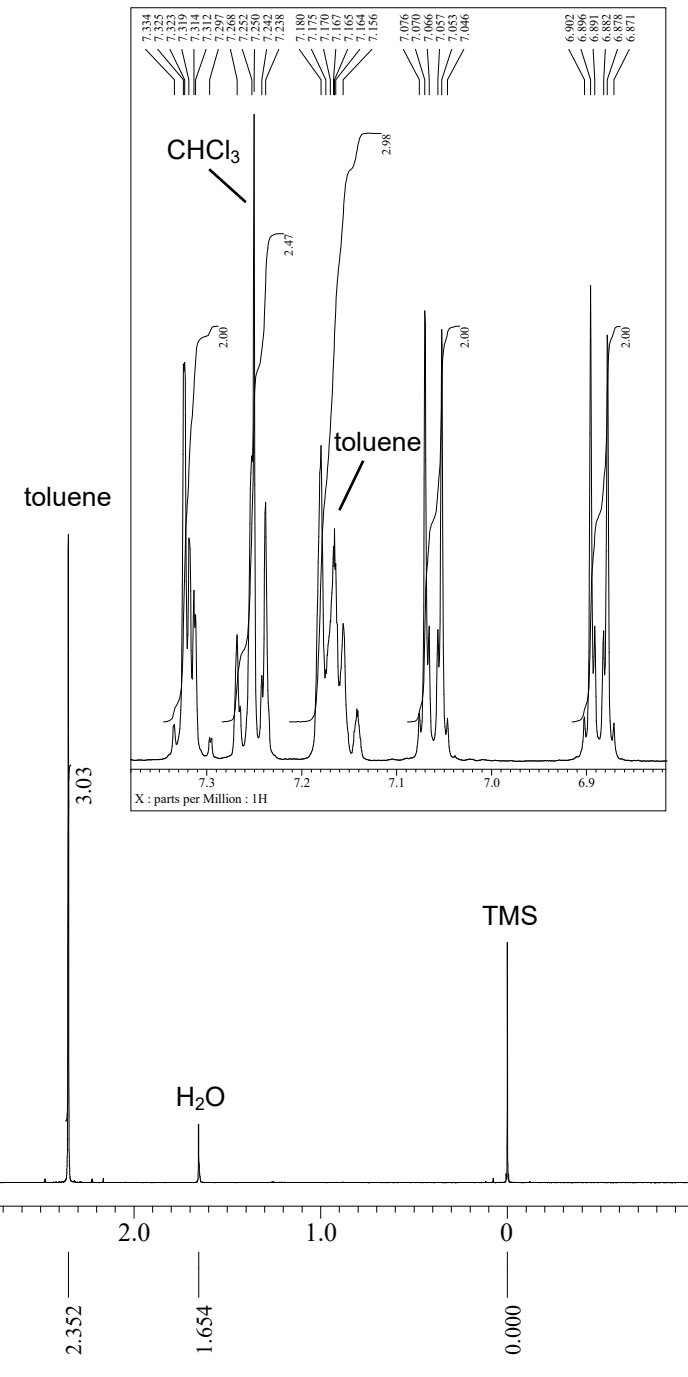
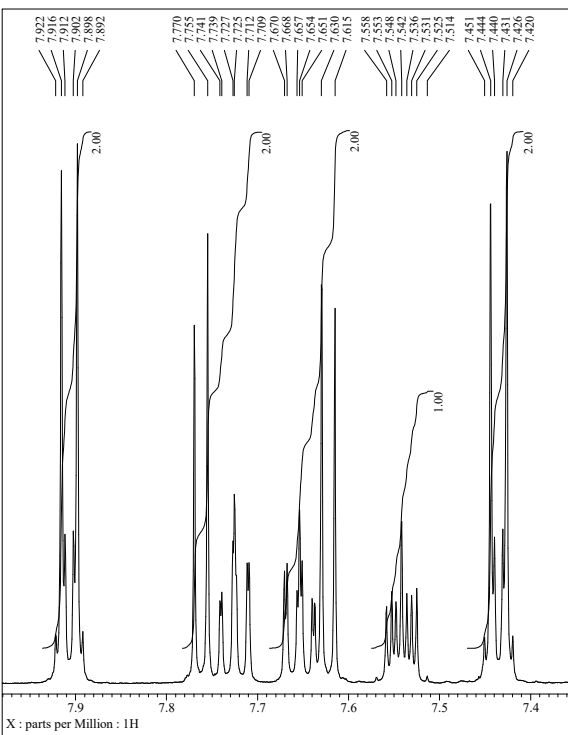
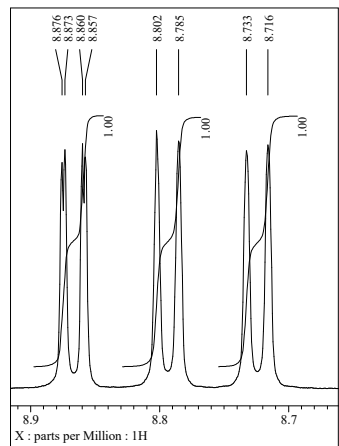
TMS



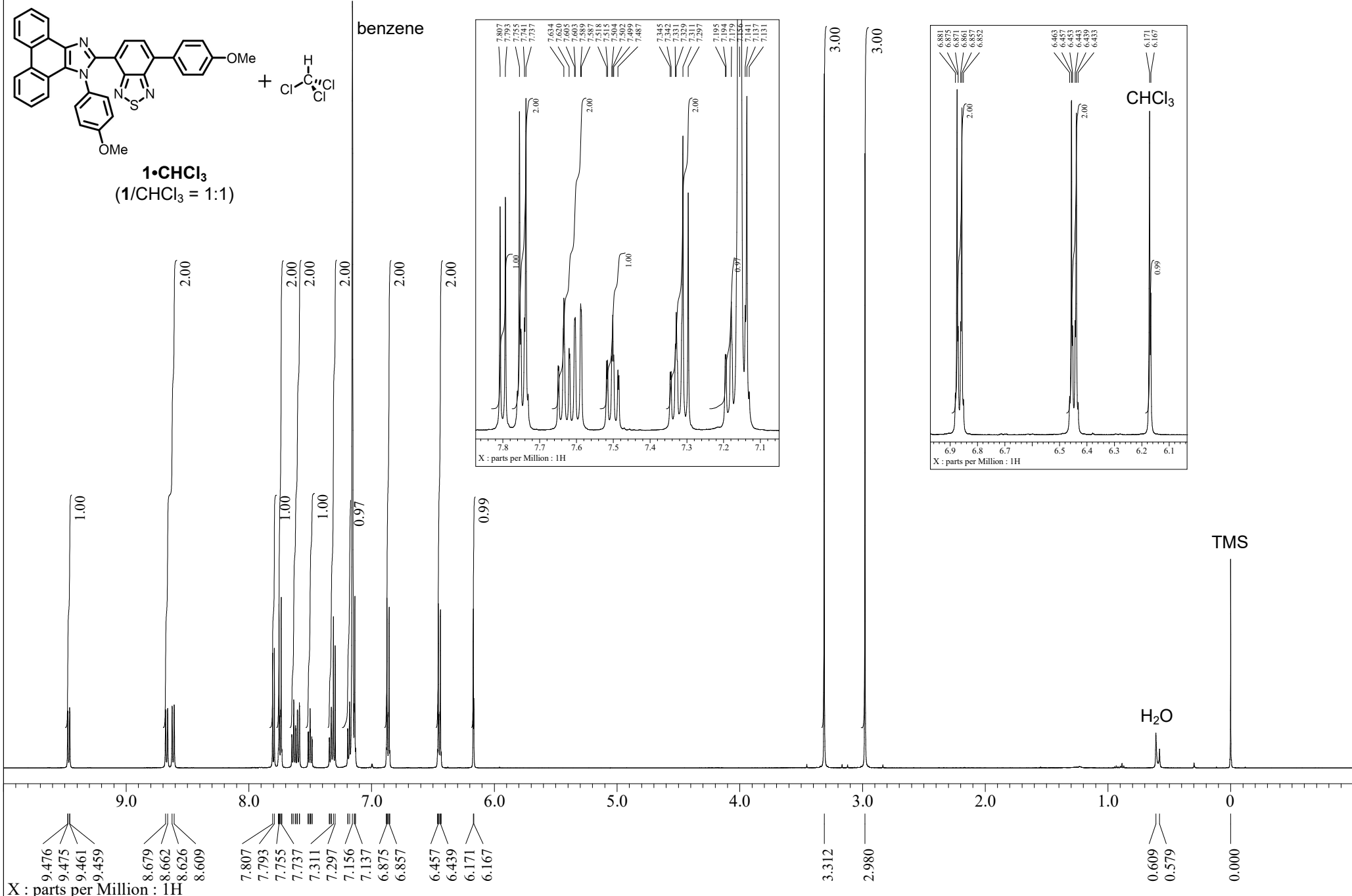
¹H NMR spectrum of 1•Toluene (500 MHz, CDCl₃, rt)



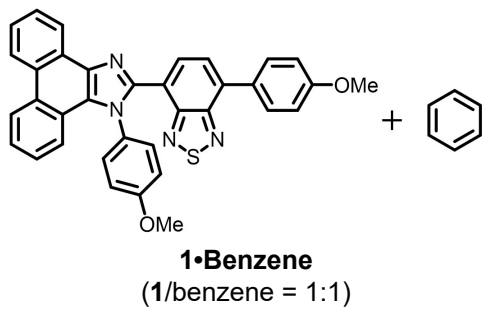
1•Toluene
(1/toluene = 1:1)



¹H NMR spectrum of 1•CHCl₃ (500 MHz, C₆D₆, rt)

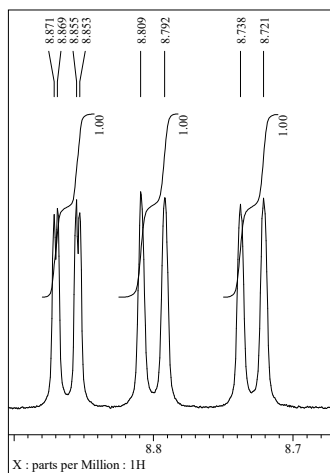


¹H NMR spectrum of 1•Benzene (500 MHz, CDCl₃, rt)

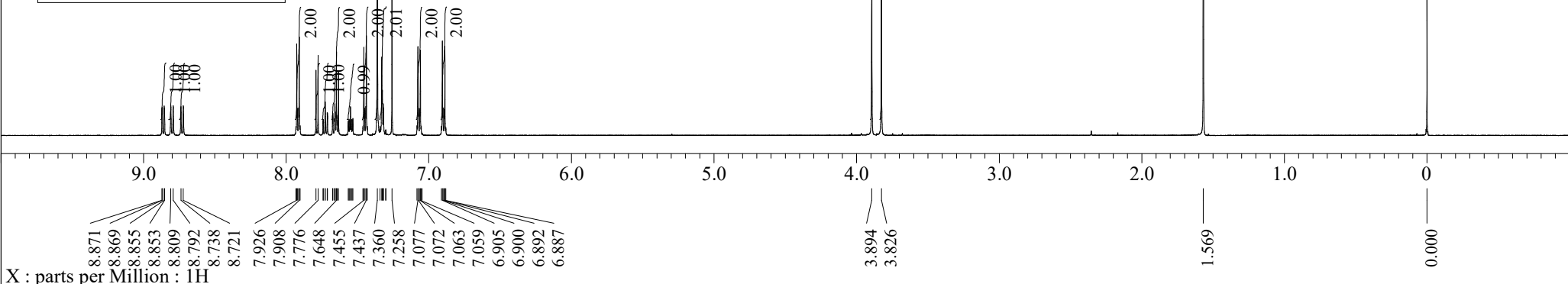


1-Benzene **(1/benzene = 1:1)**

benzene



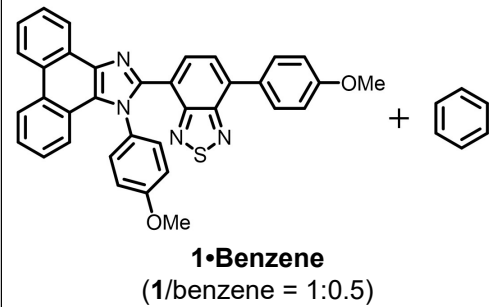
CHCl₃



H₂O

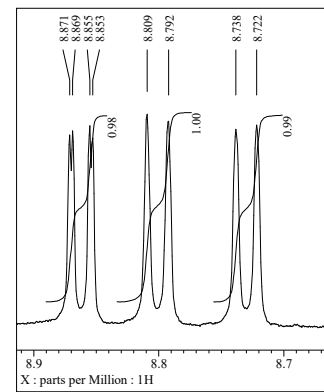
TMS

¹H NMR spectrum of ground 1•Benzene (500 MHz, CDCl₃, rt)

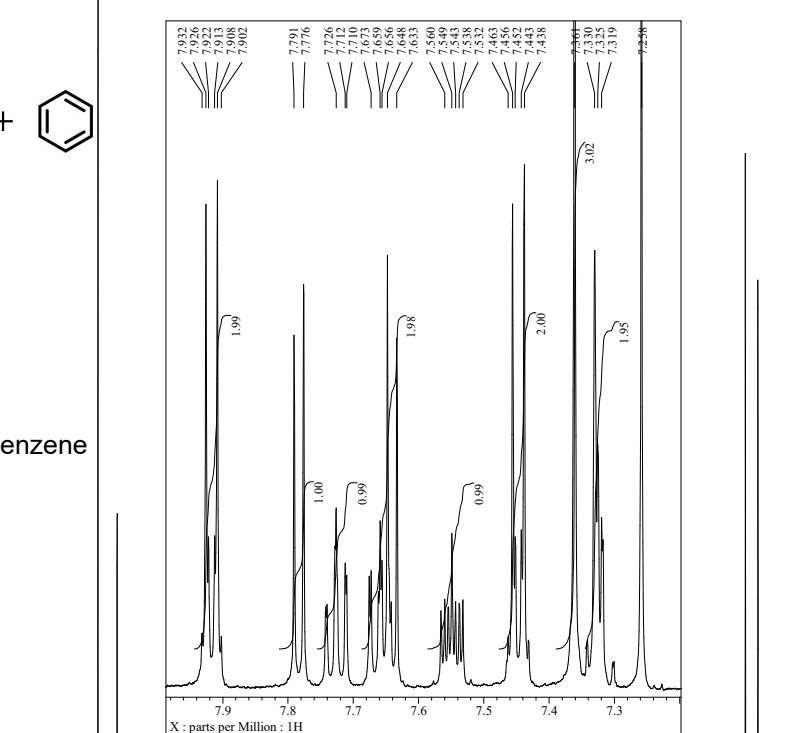


1•Benzene
(1/benzene = 1:0.5)

benzene



CHCl



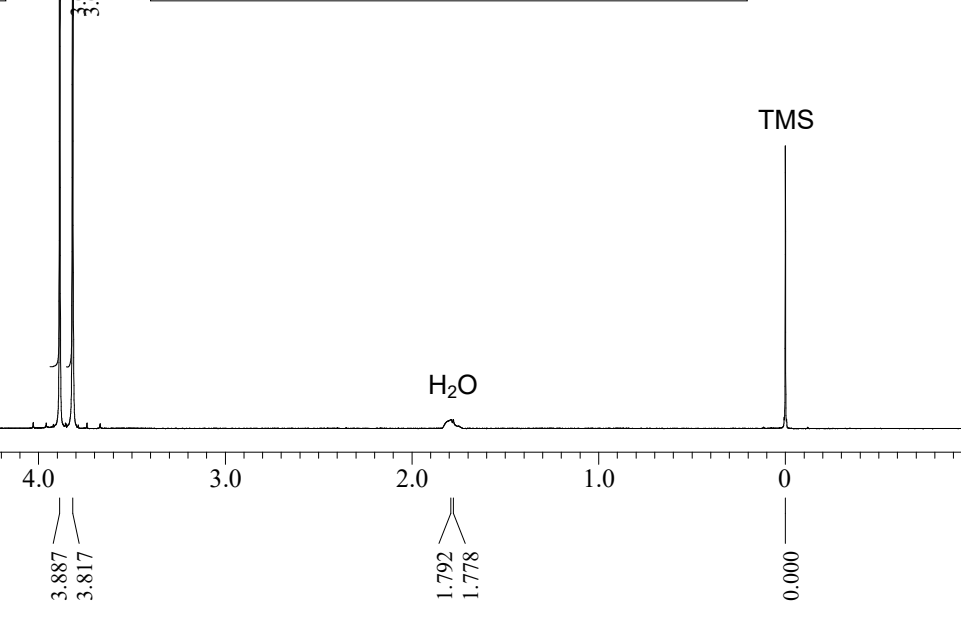
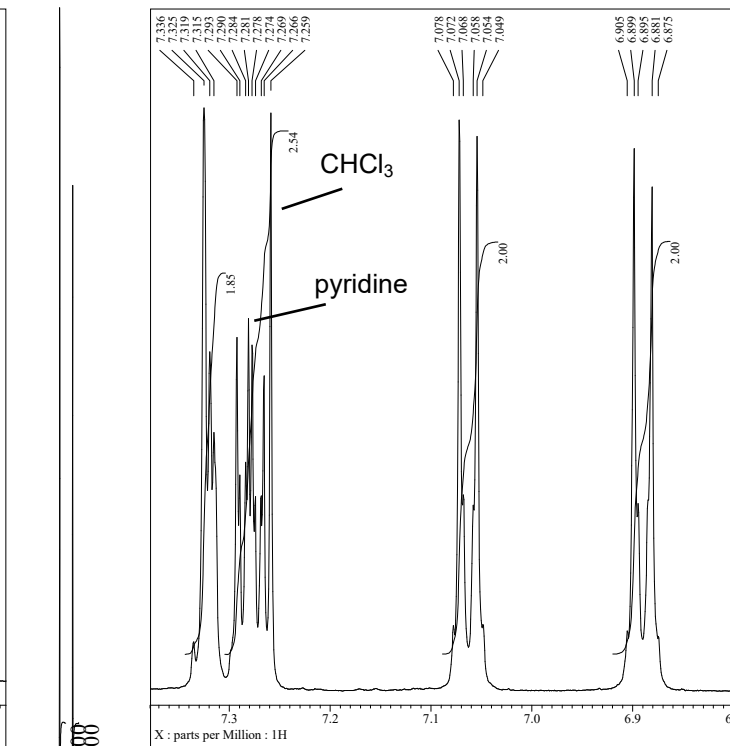
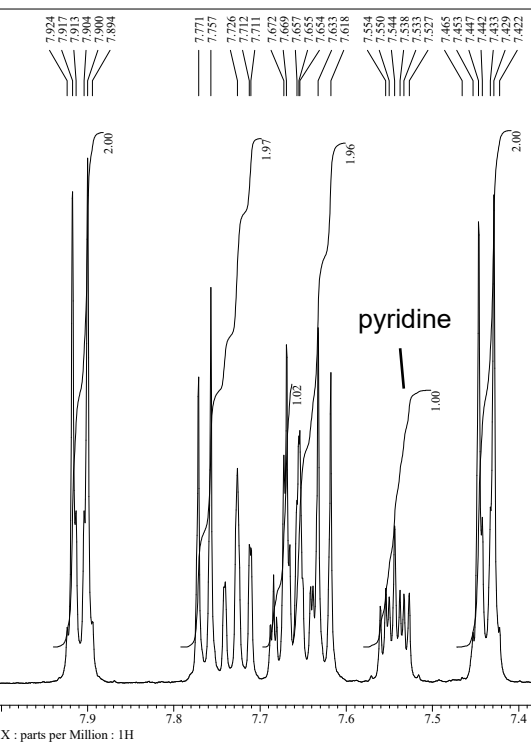
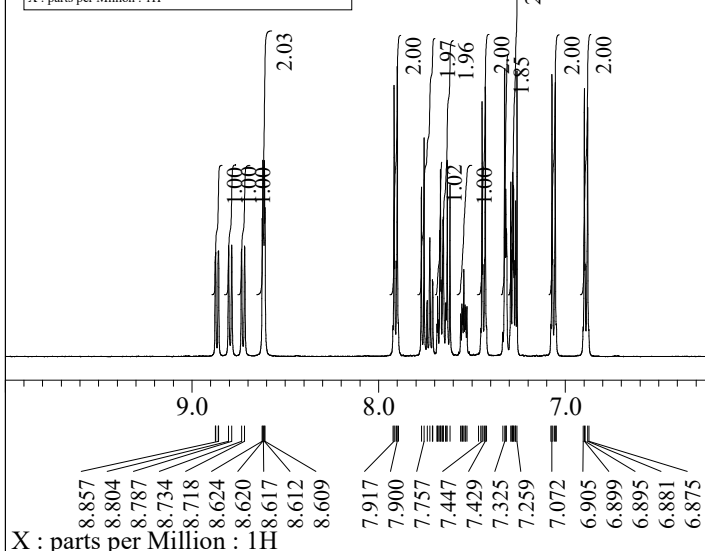
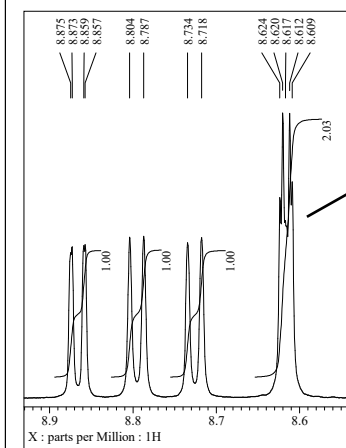
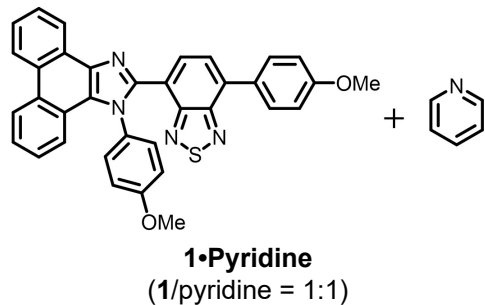
H₂O

TMS

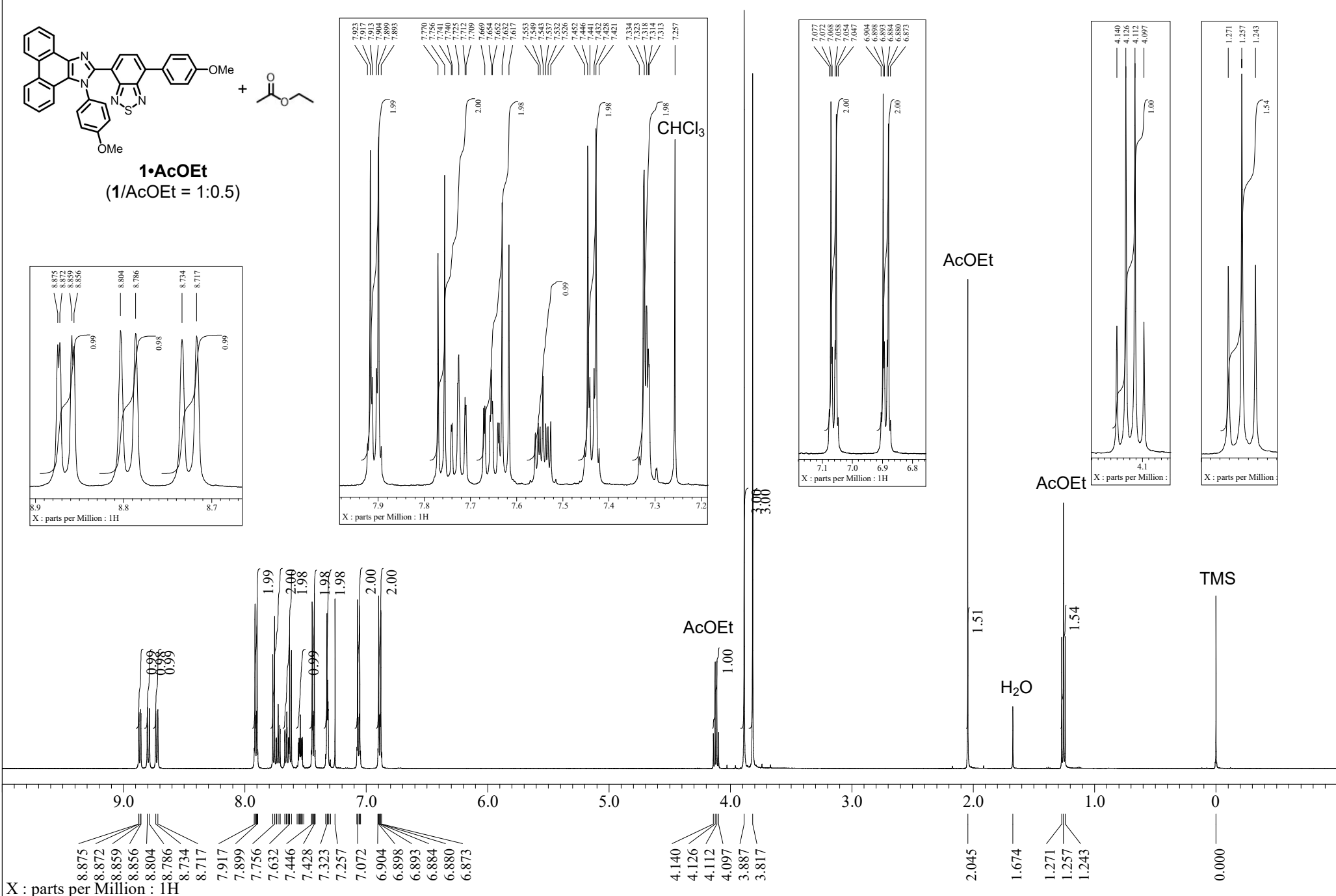


X : parts per Million : 1H

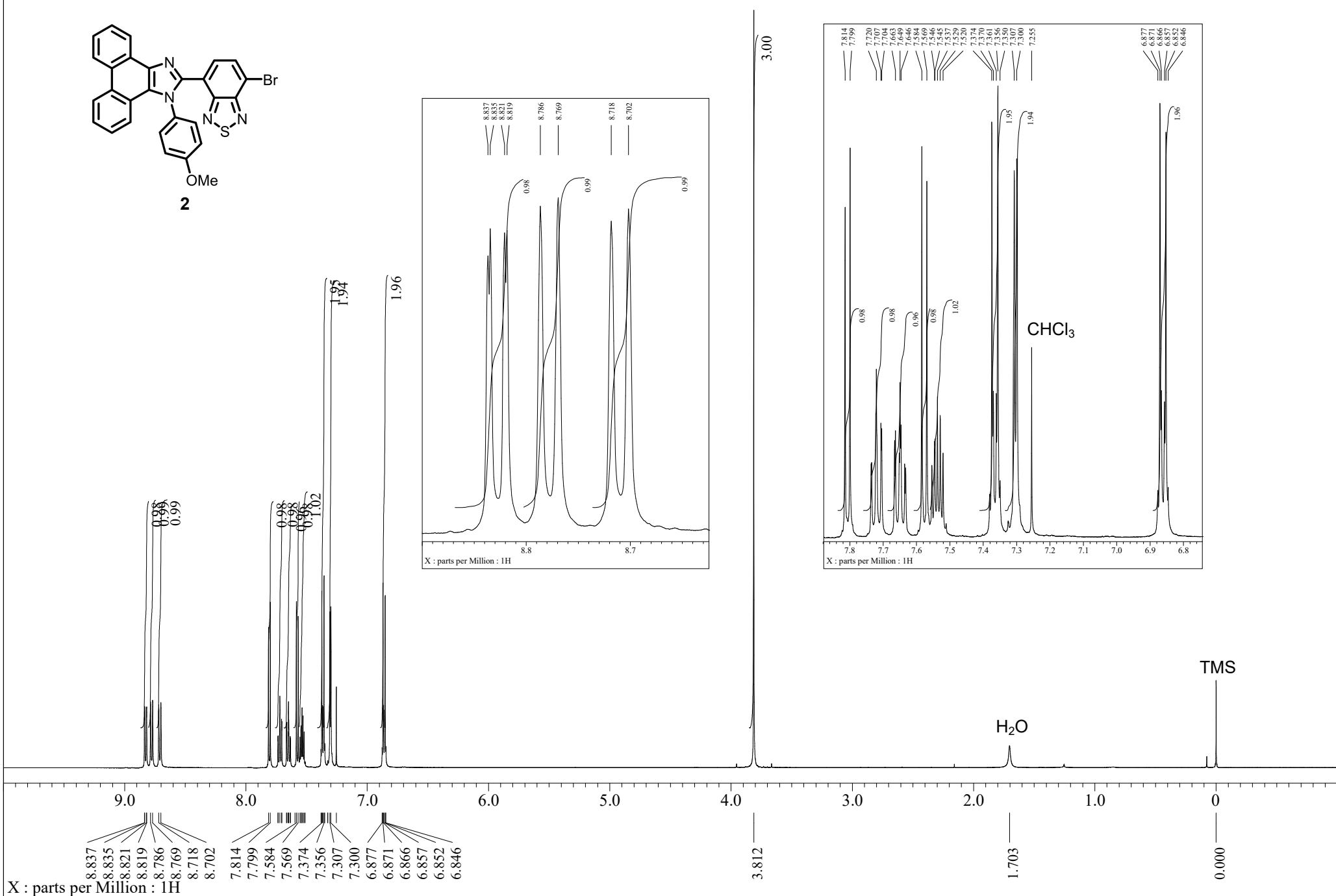
¹H NMR spectrum of 1•Pyridine (500 MHz, CDCl₃, rt)



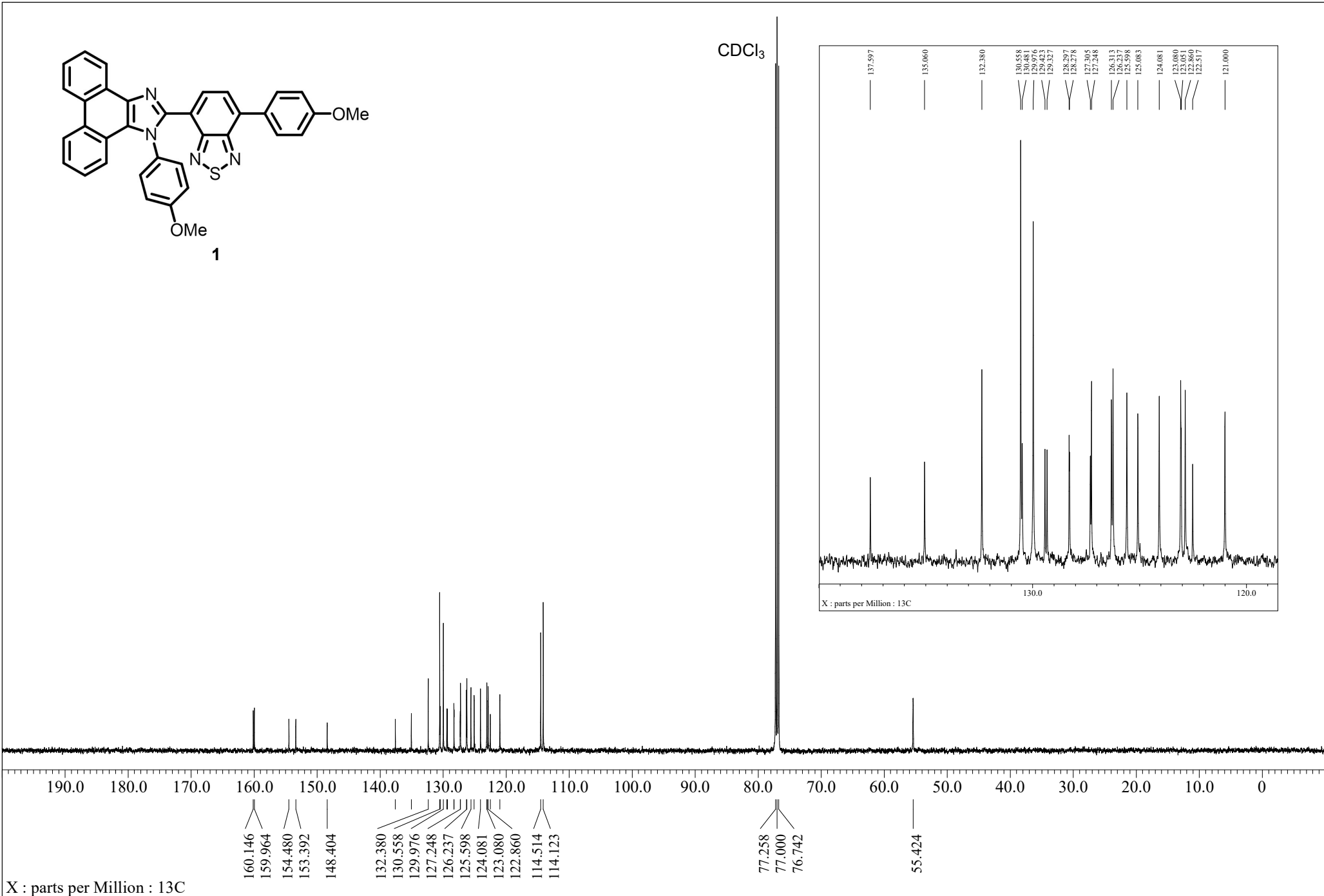
¹H NMR spectrum of 1•AcOEt (500 MHz, CDCl₃, rt)



¹H NMR spectrum of **2** (500 MHz, CDCl₃, rt)



¹³C NMR spectrum of **1** (126 MHz, CDCl₃, rt)



¹³C NMR spectrum of **2** (126 MHz, CDCl₃, rt)

